藥學碩士 學位論文

Research on Modes of Antigen Recognition by Variable Lymphocyte Receptors (VLRs)

VLRs의 항원인식 방식에 관한 연구

2013年 2月

서울大學校 大學院

藥學科 醫藥生命科學專攻

李 智 軟

Research on Modes of Antigen Recognition by Variable Lymphocyte Receptors (VLRs)

VLRs의 항원인식 방식에 관한 연구

指導敎授 韓炳憡

이 論文을 藥學碩士學位論文으로 提出 함

2012年 12月

서울大學校 大學院

藥學科 醫藥生命科學專攻

李 智 軟

李 智 軟의 藥學碩士學位論文을 認准함

2013年 1月

委 員 長 _____ (인)

副 委 員 長 _____ (인)

委 員 _____ (인)

Abstract

In jawless vertebrates, variable lymphocyte receptors (VLRs) play a crucial role in recognition of antigens as part of the adaptive immune system. Leucine-rich repeat (LRR) modules and the highly variable insert (HVI) of VLRs contribute to the specificity and diversity of antigen recognition. VLR2913, whose antigen is not known, contains the same HVI amino acid sequence with that of VLR RBC36, which recognizes the H-trisaccharide from human blood type O erythrocytes. Since the HVI sequence is rarely identical among all known VLRs, I am attempting to identify the antigen for VLR2913 and the main contributing factors for antigen recognition based on comparison of VLR2913 and VLR RBC36.

To initiate and facilitate the structural approach, the ectodomain of VLR2913 was fused with the N-terminal domain of Internalin B (InlB-VLR2913-ECD). I mutated three amino acid residues on the concave surface of LRR modules of InlB-VLR2913-ECD, considering important residues for hydrogen bonds in recognition of H-trisaccharide by VLR RBC36. The InlB-VLR2913-ECD was overexpressed in *Escherichia coli*, and crystallized at 295 K using sitting-drop vapour-diffusion methods. X-ray diffraction data were collected to 2.04 Å resolution. Crystal structure of InlB-VLR2913-ECD was determined by molecular replacement (MR).

As a reference, VLR RBC36 ectodomain was fused with N-terminus of Internalin B (InlB-VLR RBC36-ECD). InlB-VLR RBC36-ECD was overexpressed in *E. coli* and purified up to 99% purity. In binding affinity experiment by ITC200, InlB-VLR2913-ECD with 7 residues mutation, which mimicked hydrogen bonds and van der Waals interaction based on the sequence alignment between VLR RBC36 and VLR2913, showed interaction with H-trisaccharide, but wild type and three residues mutant form of InlB-VLR2913-ECD were not. I am currently trying to determine how concave surface residues influence to antigen

recognition through mutation of key factor and crystal structure of VLR2913 mutant complex with H-trisaccharide.

Keywords: variable lymphocyte receptor; VLR; adaptive immunity; antigen recognition

2011-21761

Contents

List of figures

List of tables

I. Introduction

Variable lymphocyte receptors (VLRs) recognize foreign antigens to achieve adaptive immunity in jawless vertebrates in contrast with the immunoglobulin (Ig)-type antigen receptors of jawed vertebrates (Pancer, et al., 2004, Nature, 1; Alder, et al., 2005, Science, 2). In lamprey and hagfish, the only two surviving jawless vertebrates, VLRs have been isolated by repeated injections with a cocktail of particulate antigens and mitogens (Pancer, et al., 2004, Nature, 1; Pancer, et al., 2005, Proceedings of the National Academy of Sciences of the United States of America, 3). VLRs recognize antigens using leucine-rich repeat (LRR) modules and a highly variable insert (HVI) composing the ectodomain of the functional receptor of VLRs (Han, et al., 2008, Science, 4; Velikovsky, et al., 2009, Nature structural & molecular biology, 5; Kim, et al., 2007, The Journal of biological chemistry, 6) (Fig. 1A). For diverse antigen recognition by VLRs, various numbers of the LRR modules are generated by recombinatorial DNA assembly into the vlr loci, which differs from the analogous process for antibody V, D, and J gene segments (Pancer, et al., 2004, Nature, 1; Alder, et al., 2005, Science, 2; Tasumi, et al., 2009, Proceedings of the National Academy of Sciences of the United States of America, 7). These somatic DNA rearrangements would construct a huge repertoire of about 10^{14} unique VLRs comparable to the diversity of antibody (Pancer, et al., 2004, Nature, 1). Mature VLR genes encode an N-terminal LRR capping region (LRRNT), the first LRR (LRR1), up to seven 24-residue variable LRRs (LRRVs), a terminal or end LRRV (LRRVe), a connecting peptide (CP), a C-terminal LRR capping region (LRRCT), and threonine/proline-rich stalk region that connects the protein to a glycosylphosphatidylinositol (GPI) anchor and hydrophobic tail (Han, et al., 2008, Science, 4;

Tasumi, et al., 2009, Proceedings of the National Academy of Sciences of the United States of America, 7) (Fig. 1B).

Since antibodies are known to recognize most of foreign antigens, monoclonal antibody has been used for diagnostic applications, research tools, and therapy. VLRs are important in terms of biotechnology and industry because VLRs could recognize specific antigens or pathogens (Herrin, et al., 2008, Proc Natl Acad Sci U S A, 8; Alder, et al., 2008, Nat Immunol, 9). VLRs would also be a promising monoclonal antibody alternative (Pancer and Mariuzza, 2008, Nat Biotechnol, 10). VLRs further enhance antigen-binding specificity through an HVI in LRRCT, which adopts various secondary structures and conformations (Han, et al., 2008, Science, 4; Velikovsky, et al., 2009, Nature structural & molecular biology, 5) (Fig. 1). The HVI amino acid sequence and length is important for antigen-specific interaction by VLRs (Han, et al., 2008, Science, 4; Velikovsky, et al., 2009, Nature structural & molecular biology, 5; Deng, et al., 2010, Proceedings of the National Academy of Sciences of the United States of America, 11). The amino acid sequence of the HVI is highly diverse among all known VLRs (Fig. 2). It is therefore a rare occurrence for the HVI of VLR2913 to be identical to that of VLR RBC36 which recognizes H-trisaccharide from human blood type O erythrocytes (Han, et al., 2008, Science, 4) (Fig. 3). Due to the rare identity of the HVIs between VLR2913 and VLR RBC36, H-trisaccharide or a similar glycan are potential antigen candidates for VLR2913 whose specific antigen remains undetermined. Study of binding affinity between VLR2913 and H-trisaccharide and structural study of InlB-VLR2913-ECD, according to key residues mutation, is expected to provide insights to elucidate the different modes of antigen recognition by VLRs.

I am currently attempting to discover the antigen for VLR2913, and characterize the modes of VLR antigen recognition through hypothetical interactions between VLR2913 and H-trisaccharide. To elucidate crucial factor for antigen recognition by VLRs and obtain a high level of soluble VLR2913, I designed key residues mutant forms of VLR2913 fused with Internalin B (InlB-VLR2913-ECD) which displays high thermodynamic and pH stabilities (Han, et al., 2008, Science, 4; Lee, et al., 2012, Proceedings of the National Academy of Sciences of the United States of America, 12). VLR RBC36 recognizes H-trisaccharide via hydrogen bonds by three key residues and van der Waals interaction by several residues on the concave surface (Han *et al.*, 2008) (Fig. 4). I mutated several key residues on the concave surface of LRR modules of InlB-VLR2913-ECD to mimic hydrogen bonds and van der Waals interaction based on the sequence alignment and the crystal structure of VLR RBC36 in complex with H-trisaccharide (Han *et al.*, 2008). I overexpressed the soluble InlB-VLR2913-ECD with diverse mutations in the LRR modules using *E. coli* expression system, and solubility of InlB-VLR2913-ECD varies depend on the number of mutated residue. As a reference, VLR RBC36 ectodomain was fused with N-terminus of Internalin B (InlB-VLR RBC36-ECD). InlB-VLR RBC36-ECD was overexpressed in *E. coli* and purified up to 99% purity. In binding affinity experiment by ITC200, InlB-VLR2913-ECD with 7 residues mutation, which contributing to hydrogen bonds and van der Waals interaction, was showed interaction with H-trisaccharide, but wild type and three residues mutant form of InlB-VLR2913-ECD were not. In this report, I describe the cloning, mutagenesis, overexpression, purification, crystallization, x-ray diffraction data collection, crystal structure and binding affinity by ITC200.

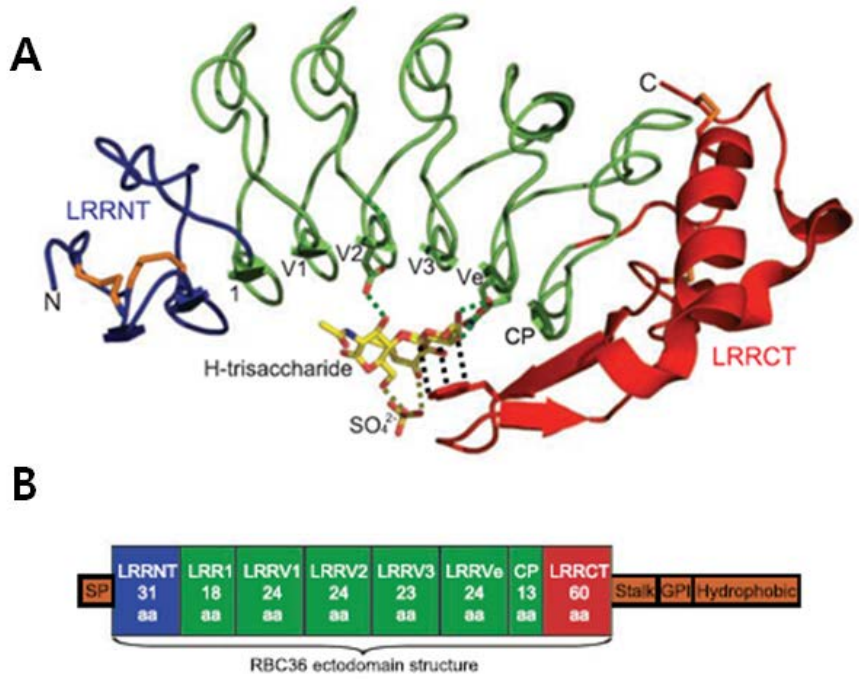

Figure 1. Overall architecture of the VLR RBC36-ECD in complex with the H-trisaccharide.

(A) Ribbon diagram of RBC36-ECD in complex with H-trisaccharide LRRNT, LRRs, and LRRCT are colored blue, green, and red, respectively. Carbons, nitrogens, and oxygens of the H-trisaccharide are colored yellow, blue, and red, respectively. Disulfide bridges are shown in orange. Green dotted lines represent hydrogen bonds; black dotted lines indicate hydrophobic effects. [Protein Data Bank (PDB) ID 3E6J] (Han, et al., 2008, Science, 4).

(B) Schematic diagram of RBC36. Regions from left to right: signal peptide (SP), N-terminal LRR (LRRNT), five variable LRRs (LRR1, LRRVs), connecting peptide (CP), C-terminal LRR (LRRCT), threonine/proline-rich stalk region,GPI anchor, and hydrophobic tail. (Han, et al., 2008, Science, 4).

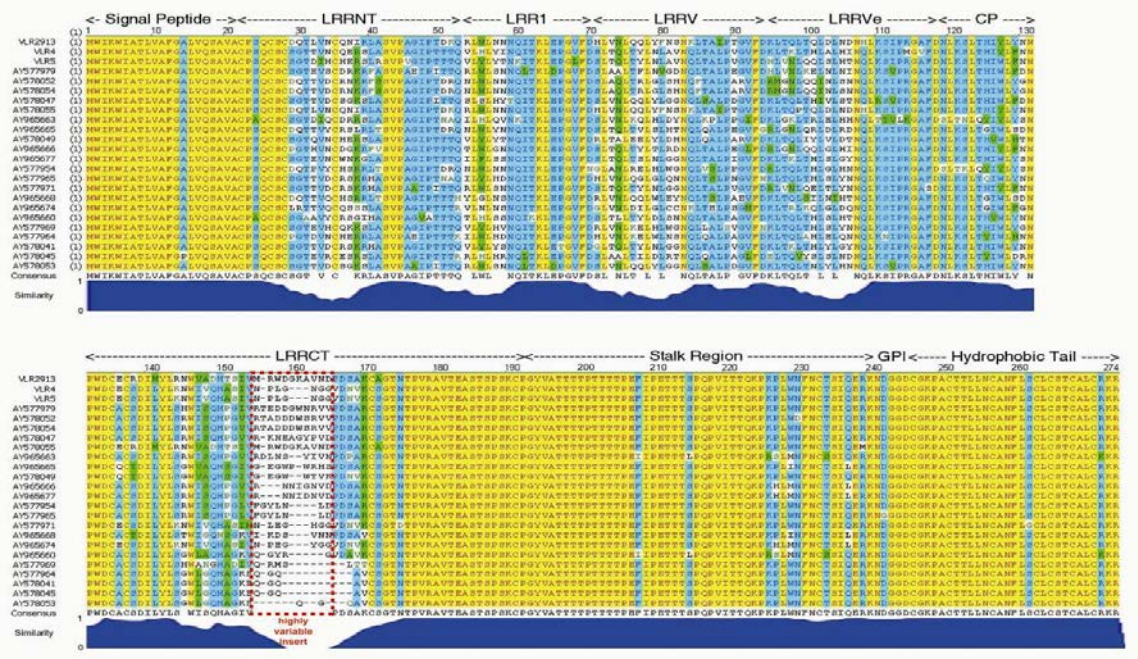

Figure 2. Sequence alignment of VLR2913, VLR4, VLR5, and 21 other lamprey VLRs.

All VLRs shown here contains one LRRV and almost the same sequences for the signal peptide, connecting peptide, GPI anchor region, and hydrophobic tail. VLRs, except VLR2913, VLR4, and VLR5, are labeled as the GenBank accession number (AY#). Identical residues are shown as red letters on yellow background; conserved residues are blue on cyan; similar residues are black on green; non-similar residues are black on white. In the similarity graph on the bottom, the insert in LRRCT shows that the composition and length of amino acids are highly variable

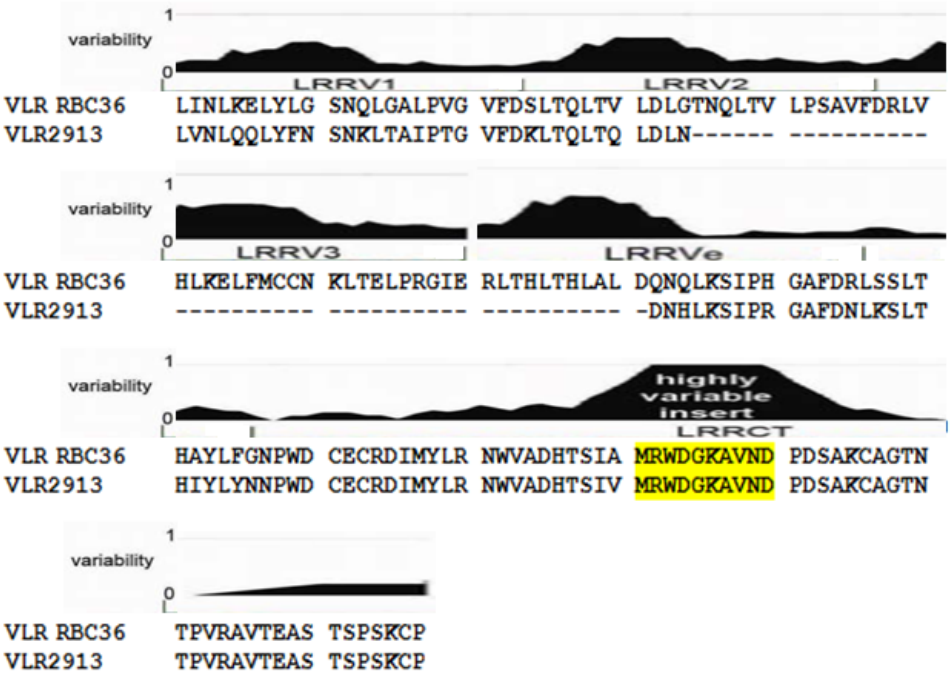

Figure 3. Sequence alignment of VLR RBC36 and VLR2913.

Yellow mark shows sequence identity of highly variable insert between VLR RBC36 and VLR2913.

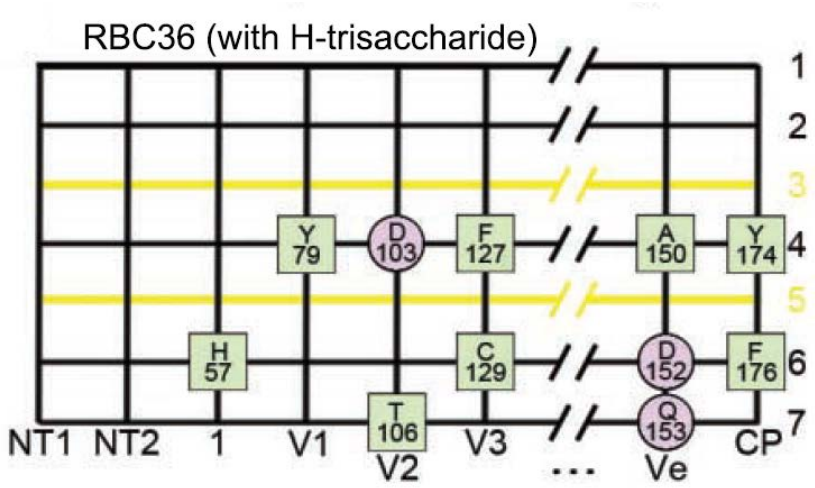

Figure 4. The Interaction matrix of VLRs.

Residues involved in hydrogen bonds or in van der Waals contacts are labeled in a circle or in a square, respectively (Han, et al., 2008, Science, 4).

Ⅱ. Materials and methods

1. Materials

InlB gene synthesis and polymerase chain reaction (PCR) primers, which are used for VLR gene amplification, were purchased from IDT and Cosmogene tech (Seoul, Korea), respectively. Luria Broth (LB) medium and Ampicillin were purchased from Sigma Aldrich. Restriction enzymes (*Nde*I, *BamH*I and *Xho*I) were purchased from Enzynomics, Korea). The expression vector pET-21a(+), *E. coli* BL21- CodonPlus(DE3)-RIPL cells and Rosetta2(DE3) were obtained from Novagen (Darmstadt, Germany) and nnn, respectively.

2. Methods

2.1. Cloning

2.1.1 VLR2913 Cloning

The LRRV1 to LRRCT (residues 72-191) of the VLR2913 was amplified, and the one forward and one reverse oligonucleotide primers are 5'-CAGCGCGCTGGGATCCCTGGTGAATCTGCAGCAG-3' (Forward)' and 5'-GGTGGTGGTGCTCGAGTGGGCATTTCGAGGGGCTA-3'(Reverse). The amplified DNA was inserted into the expression vector pET21a(+) (Novagen) using infusion kit, and the N-terminal domain (81 amino acid) of Internalin B was fused to the N-terminus of VLR2913 (Lee, et al., 2012, Proceedings of the National Academy of Sciences of the United States of America, 12) (InlB-VLR2913-ECD). This vector construction adds a hexa-histidine containing tag (LEHHHHHH) to the C-terminus of the VLR2913 gene product to facilitate protein purification.

2.1.2 VLR RBC36 Cloning

The LRRV1-LRRCT (residues 54-238), LRRV2-LRRCT (residues 95-238), LRRV3-LRRCT (residues 120-238) and LRRVe-LRRCT (residues 143-238) of the VLR RBC36 were amplified, and the four forward and one reverse oligonucleotide primers are 5'-CAGCGCGCTGGGATCCCTCATAAATCTGAAGGAGCTGTATC-3' (residues 54-238), 5'-CAGCGCGCTGGGATCCCTGACGCAA CTTACTGTCCTG-3' (residues 95-238), 5'-CAGCGCGCTGGGATCCCTGGTGCATCTAAAAGAGCTG-3' (residues 120-238), 5'-CAGCGCGCTGGGATCCCTCACCCATTTGACTCATTTAGC-3' (residues 143-238) and

5’- GGTGGTGGTGCTCGAGTGGGCATTTCGA GGGGCTA-3’(Reverse). The amplified DNA was inserted into the expression vector pET21a(+) (Novagen) using infusion kit, and the N-terminal domain (81 amino acid) of Internalin B was fused to the N-terminus of VLR RBC36 (Lee, et al., 2012, Proceedings of the National Academy of Sciences of the United States of America, 12) (InlB-VLR RBC36-ECD). This vector construction adds a hexa-histidine containing tag (LEHHHHHH) to the C-terminus of the VLR RBC36 gene product to facilitate protein purification.

2.2. Mutagenesis

The mutation of residues in the LRR modules of InlB-VLR2913-ECD was prepared with the QuikChange II Site-Directed Mutagenesis Kit (Stratagene, La Jolla, CA, USA). The 12 mutant forms of InlB-VLR2913-ECD were designed by comparison with key residues involved in hydrogen bonds and van der Waals interaction for recognition between VLR RBC36 and H-trisaccharide. The 9 forward and 9 reverse oligonucleotide primers for mutagenesis of InlB-VLR2913-ECD are in the below table 1.

A70D	Forward	5’-GCCGAATGTGCGTTATTTGGACCTGGGTGGCAATAAACTG-3’
	Reverse	5’-CAGTTTATTGCCACCCAGGTCCAAATAACGCACATTCGGC-3’
N118D	Forward	5’-GCTCACTCAACTGGATTTGGATGACAACCATCTGAAGAG-3’
	Reverse	5’-CTCTTCAGATGGTTGTCATCCAAATCCAGTTGAGTGAGC-3’
D119Q	Forward	5’-CTCAACTGGATTTGAATCAGAACCATCTGAAGAGCATTCCC-3’
	Reverse	5’-GGGAATGCTCTTCAGATGGTTCTGATTATCCAGTTGAG-3’
N118D_D119Q	Forward	5’-CTCACTCAACTGGATTTGGATCAGAACCATCTGAAGAGCATTCCC-3’
	Reverse	5’-GGGAATGCTCTTCAGATGGTTCTGATCCAAATCCAGTTGAGTGAG-3’
I48Y	Forward	5’-GAACGAACTGAACTCGATCGATCAAATCTATGCGAATAATAGCG-3’
	Reverse	5’-CGCTATTATTCGCATAGATTTGATCGATCGAGTTCAGTTCGTTC-3’
G73T	Forward	5’-GCGTTATTTGGACCTGGGTACCAATAAACTGCATGACATCAG-3’
	Reverse	5’-CTGATGTCATGCAGTTTATTGGTACCCAGGTCCAAATAACGC-3’
Y92F_N94C	Forward	5’-GGTGAATCTGCAGCAGCTCTTTTTTTGCAGCAACAAGCTAACAGC-3’
	Reverse	5’-GCTGTTAGCTTGTTGCTGCAAAAAAAGAGCTGCTGCAGATTCACC-3’
D116A	Forward	5’-CAGCTCACTCAACTGGCTTTGGATCAGAACCATC-3’
	Reverse	5’-GATGGTTCTGATCCAAAGCCAGTTGAGTGAGCTG-3’
Y142F	Forward	5’-CTAACTCACATCTATCTGTTCAACAACCCATGGGATTGC-3’
	Reverse	5’-GCAATCCCATGGGTTGTTGAACAGATAGATGTGAGTTAG-3’

Table 1. Forward and reverse primers for mutagenesis of InlB-VLR2913-ECD

2.3. Overexpression

The recombinant protein was overexpressed in *Escherichia coli* BL21 (DE3) RIPL cells. Cells were grown at 310 K up to OD_{600} of 0.8 in Luria Broth culture medium containing 50 mg ml^{-1} amphicillin and the protein expression was induced by 0.5 m*M* isopropyl 1-thio-β-D-galactopyranoside (IPTG). The cells were continued to grow at 293 K for 16 h after IPTG induction and were harvest by centrifugation at 6,000 g for 10 min at 277 K.

2.4. Purification

2.4.1 Cell lysis

The cell pellets were lysed by sonication in buffer A (20 mM Tris-HCl at pH 7.5, 500 mM NaCl, and 35 mM imidazole) containing 1 mM phenylmethylsulfonyl fluoride (PMSF). The crude lysate was centrifuged at 36,000 g for 1 hr at 277 K and the cell debris was discarded. The same process has done for all the proteins.

2.4.2 Column chromatography and Concentration

The first step for purification of InlB-VLR2913-ECD mutant forms and InlB-VLR RBC36-ECD utilized the C-terminal hexa-histidine tag by affinity chromatography on HiTrap chelating HP column (GE Healthcare, Little Chalfont, UK), which was previously charged with 50 mM $NiSO_4$ and equilibrated with 20 m*M* Tris-HCl at pH 7.5, 500 m*M* NaCl, and 35 m*M* Imidazole. As a second step, gel filtration was performed on a HiLoad 16/600 Superdex 200 prep-grade column (GE Healthcare), which was previously equilibrated with 20 mM Tris-HCl at pH 8.5 and 100 mM NaCl. Lastly, anion exchange was done using HiTrap Q ion-exchange column (GE Healthcare, Little Chalfont, UK). Homogeneity of the purified protein was assessed by sodium dodecyl sulfate-polyacrylamide gel electrophoresis (SDS-PAGE). Purified protein was concentrated using an Amicon Ultra-3K centrifugal filter device (Millipore, Billerica, MA, USA). The protein concentration was calculated by bicinchoninic acid assay **(**BCA assay**).**

2.5. Crystallization

Initial screening was performed at 295 K by the sitting-drop vapour-diffusion method using 96-well crystallization plates. Each sitting drop was prepared by mixing 1 µl of the protein solution (20.0 mg ml^{-1} protein concentration in final purified buffer with 20 mM Tris-HCl at pH 8.5 and 100mM NaCl) and 1 µl of the reservoir solution, and was placed over 100 µl reservoir solution. Commercially available crystallization kits such as Structure Screen 1, Structure Screen 2 (Moleculardimensions), Wizard classic 1, Wizard classic 2, Wizard classic 3, Wizard classic 4 (Emerald BioSystems), MIDAS (Moleculardimensions) and The Classics Suite (Qiagen) were used for initial. Optimization was performed at 295 K by sitting-drop vapour-diffusion methods using 24-well crystallization plates. Each sitting drop was prepared by mixing 1.5 µl of the protein solution (20.0 mg ml-1 protein concentration in buffer with 20 mM Tris-HCl at pH 8.5 and 100mM NaCl) and 1.5 µl of the reservoir solution, and was placed over 500 µl reservoir solution. The crystallization condition is 0.17 *M* ammonium sulfate, 25.5%(*w/v*) PEG 4000 and 15%(*v/v*) glycerol (No. 30, Wizard III, Emerald Biosystems, Bainbridge Island, WA, USA).

2.6. X-ray data collection

No further cryoprotectant was required for cryo-cooling in liquid nitrogen. X-ray diffraction data were collected at 100 K using a MicroMax-007 HF microfocus x-ray generator and an R-AXIS IV^{++} imaging-plate area detector (Rigaku, Tokyo, Japan) at the Korea Basic Science Institute (KBSI), Korea. Table 1 summarizes the statistics for data collection. For each image, the crystal was rotated by 1° and the raw data were processed using the program suite HKL2000 (Otwinowski and Minor, 1997, Method Enzymol, 13).

2.7. Structure determination

The crystal structure was determined by molecular replacement (MR) and with the program Molrep-autoMR. Two search model (Protein Data Bank, PDB ID: 3RFJ and 2R9U) were selected from the PDB data base.

2.8. Isothermal Titration Calorimetry 200

Isothermal titration calorimetry (ITC) is a technique used to study the binding of small molecules to larger macromolecules. The interaction between InlB-VLR2913-ECD/InlB-VLR RBC36-ECD and H-trisaccharide was measured at 293 K using ITC200 on condition that molar ratio of 10:1 and 20:1 (H-trisaccharide : InlB-VLR2913-ECD). Each 2 μl of H-trisaccharide was injected 20 times into buffer (20 mM Tris-HCl at pH 8.5 and 100 mM NaCl) containing InlB-VLR2913-ECD in duration time of 4 sec and spacing of 150 sec.

III. Results and discussion

1. Cloning

The LRRV1 to LRRCT (residues 72-191) of the VLR2913 ectodomain was constructed as a fusion protein with Internalin B (InlB-VLR2913-ECD), to facilitate biochemical and structural approach. The LRRV1-LRRCT (residues 54-238), LRRV2-LRRCT (residues 95-238), LRRV3-LRRCT (residues 120-238) and LRRVe-LRRCT (residues 143-238) of the VLR RBC36 ectodomain were fused with N-terminus of Internalin B (InlB-VLR RBC36-ECD).

2. Mutagenesis

The 12 mutant forms of InlB-VLR2913-ECD were A70D, N118D**,** D119Q, A70D_N118D, A70D_D119Q, N118D_D119Q, A70D_N118D_D119Q, A70D_N118D_D119Q_Y142F, A70D_N118D_D119Q_D116A_Y142F, A70D_N118D_D119Q_Y92F_N94C_D116A_ Y142 F, A70D_N118D_D119Q_G73T_Y92F_N94C_D116A_Y142F and A70D_N118D_ D119Q _I48Y_ G73T_Y92F_N94C_D116A_Y142F.

3. Overexpression

3.1 InlB-VLR2913-ECD Overexpression

The InlB-VLR2913-ECD and mutant forms were successfully overexpressed in an *E. coli* BL21(DE3)RIPL. The expression level and solubility of InlB-VLR2913-ECD varies depend on the number of mutated residue (Figure 5). For example, the expression level of InlB-VLR2913-ECD with 9 mutated residues was lowest among all InlB-VLR2913-ECD mutant forms.

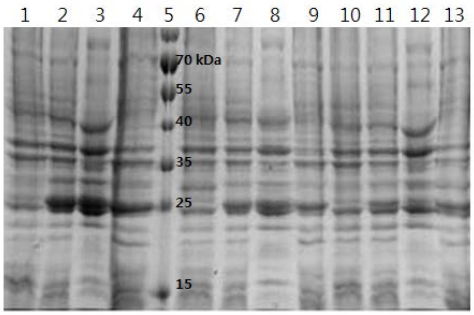

Figure 5. SDS-PAGE of expression and solubility test at 293 K

A) A70D_N118D_D119Q_D116A_Y142F
B) A70D_N118D_D119Q_ Y92F_N94C_D116A_Y142F
C) A70D_N118D_D119Q_I48Y_ G73T _Y92F_N94C_D116A_Y142F
Lane 1: **A**, Before induction
Lane 2: **A**, Post induction
Lane 3: **A**, Supernatant fraction
Lane 4: **A**, Precipitant fraction
Lane 5: Protein marker (Fermentas)
Lane 6: **B**, Before induction
Lane 7: **B**, Post induction
Lane 8: **B**, Supernatant fraction
Lane 9: **B**, Precipitant fraction
Lane 10: **C**, Before induction
Lane 11: **C**, Post induction
Lane 12: **C**, Supernatant fraction
Lane 13: **C**, Precipitant fraction

3.2 InlB-VLR RBC36-ECD Overexpression

The InlB-VLR RBC36-ECD was overexpressed in an *E. coli* Rosetta2(DE3) and BL21(DE3)RIPL. The expression level and solubility of InlB-VLR RBC36-ECD varies depend on constructs (Figure 6). For example, the LRRV3-LRRCT (residues 120-238) of InlB-VLR RBC36-ECD construct was not expressed in *E. coli* (Figure 6B).

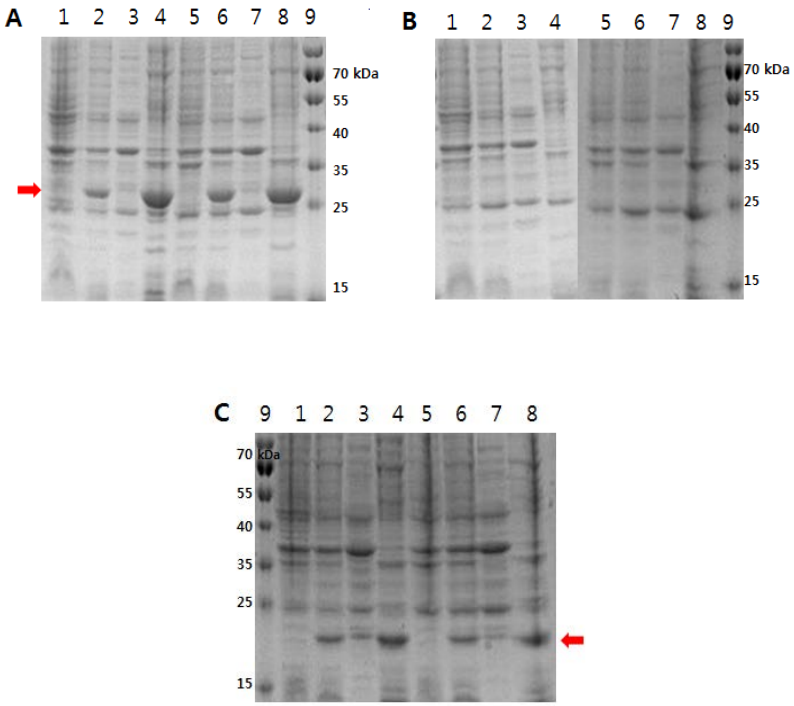

Figure 6. SDS-PAGE of expression and solubility test at 293 K

(A) LRRV2-LRRCT, (B) LRRV3-LRRCT, (C) LRRVe-LRRCT

Lane 1: Before induction, Rosetta2 (DE3)
Lane 2: Post induction, Rosetta2 (DE3)
Lane 3: Supernatant fraction, Rosetta2 (DE3)
Lane 4: Precipitant fraction, Rosetta2 (DE3)
Lane 5: Before induction, BL21 (DE3) RIPL
Lane 6: Post induction, BL21 (DE3) RIPL
Lane 7: Supernatant fraction, BL21 (DE3) RIPL
Lane 8: Precipitant fraction, BL21 (DE3) RIPL
Lane 9: Protein marker (Fermentas)

4. Purification

4.1 InlB-VLR2913-ECD Purification

4.1.1 InlB-VLR2913-ECD (Wild type) Purification

The induced cells were harvested by centrifugation at 6,000 g for 10 min at 277 K. The wet cell weight was about 11.5 g for 4.5L culture. The cell pellets were lysed by sonication in buffer A (20 mM Tris-HCl at pH 7.5, 500 mM NaCl, 35 mM imidazole) containing 1 mM PMSF. The crude cell extract was centrifuged at 36,000 g for 1 hr at 277 K and the cell debris was discarded. The first step utilized the N-terminal hexa-histidine tag by affinity chromatography on a HiTrap chelating HP column (GE Healthcare), which was previously charged with 50 mM $NiSO_4$ and equilibrated with buffer A. The protein was eluted with buffer A containing 1 M imidazole. Figure 7 shows the elution profile from the HiTrap chelating HP column and SDS-PAGE of column fractions is shown in Figure 8. Secondly, gel filtration was performed on a HiLoad 16/600 Superdex 200 prep-grade column (GE Healthcare) with an elution buffer of 20 mM Tris-HCl at pH 8.0 and 100 mM NaCl. Figure 9 shows the elution profile of Superdex 200 column and SDS-PAGE of column fractions is displayed in Figure 10. Anion exchange chromatographic step was performed on HiTrap Q HP column, which was previously equilibrated with buffer (20 mM Tris-HCl at pH 8.0, 100 mM NaCl). VLR protein was eluted during sample loading (Figure 11). The purified proteins were homogeneous as judged by SDS-PAGE analysis (Figure 12)..

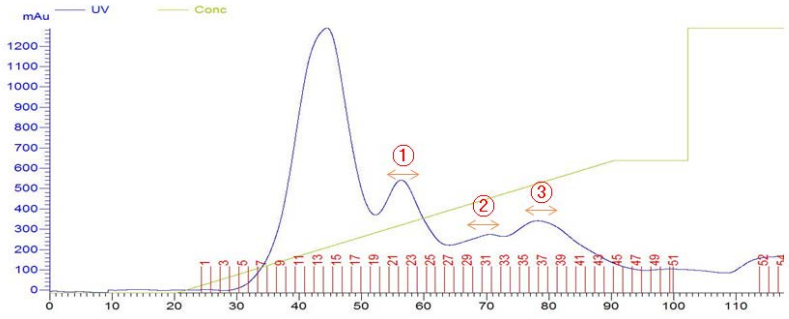

Figure 7. Elution profile from the HiTrap chelating HP column chromatography

Elution was performed with a linear gradient of 35 mM to 500 mM imidazole in 20 mM Tris-HCl at pH 7.5, and 500 mM NaCl

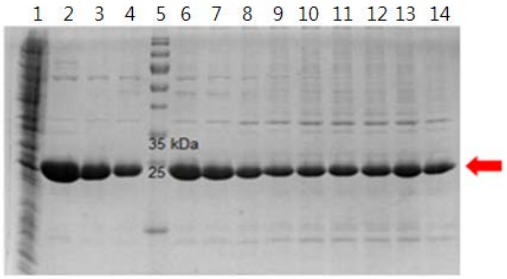

Figure 8. SDS-PAGE analysis of HiTrap chelating HP column fractions

Lane 1: Loading-thru
Lane 2: fraction #13
Lane 3: fraction #17
Lane 4: fraction #19
Lane 5: Protein marker (Fermentas)
Lane 6: fraction #21
Lane 7: fraction #23
Lane 8: fraction #25
Lane 9: fraction #27
Lane 10: fraction #29
Lane 11: fraction #31
Lane 12: fraction #33
Lane 13: fraction #35
Lane 14: fraction #40

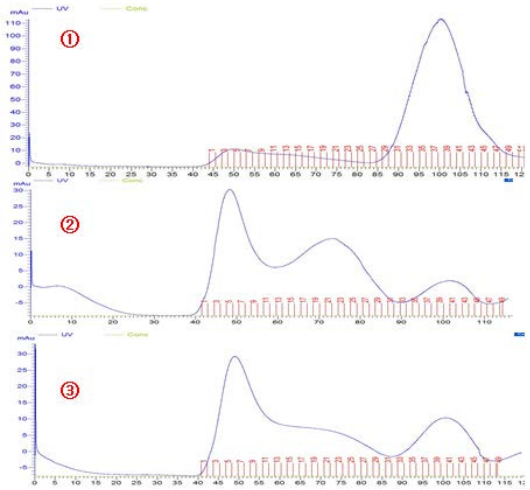

Figure 9. Elution profile from the Superdex-200 column chromatography

Elution was performed with 20 mM Tris-HCl at pH 8.0 and 100 mM NaCl

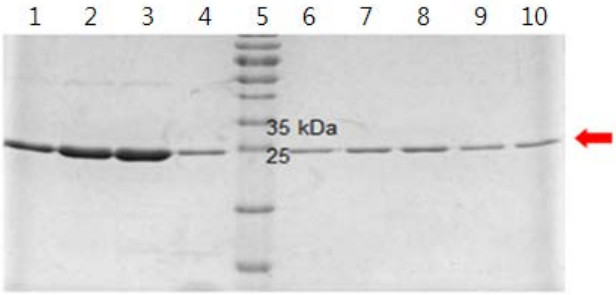

Figure 10. SDS-PAGE analysis of Superdex-200 column fractions

Lane 1: Elution profile① fraction #30
Lane 2: Elution profile① fraction #33
Lane 3: Elution profile① fraction #37
Lane 4: Elution profile① fraction #45
Lane 5: Protein marker (Fermentas)
Lane 6: Elution profile② fraction #34
Lane 7: Elution profile② fraction #36
Lane 8: Elution profile② fraction #38
Lane 9: Elution profile③ fraction #36
Lane 10: Elution profile③ fraction #39

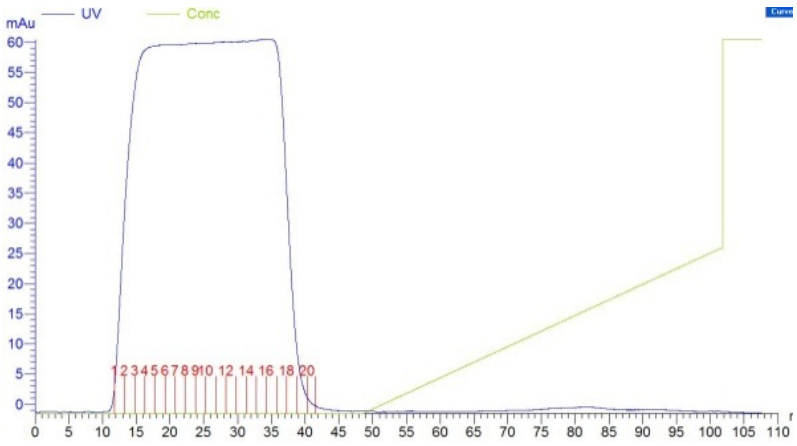

Figure 11. Elution profile from the HiTrap Q HP column chromatography

Elution was performed with a linear gradient of 100 mM to 500 mM NaCl in 20 mM Tris-HCl at pH 8.0

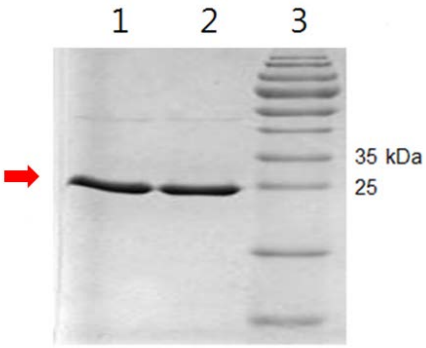

Figure 12. SDS-PAGE analysis of HiTrap Q HP column fractions

Lane 1: fraction #5
Lane 2: fraction #16
Lane 3: Protein marker (Fermentas)

4.1.2 InlB-VLR2913-ECD (A70D_N118D_D119Q) Purification

The induced cells were harvested by centrifugation at 6,000 g for 10 min at 277 K. The wet cell weight was about 15.5 g for 4.5L culture. The cell pellets were lysed by sonication in buffer A (20 mM Tris-HCl at pH 7.5, 500 mM NaCl, 35 mM imidazole) containing 1 mM PMSF. The crude cell extract was centrifuged at 36,000 g for 1 hr at 277 K and the cell debris was discarded. The first step utilized the N-terminal hexa-histidine tag by affinity chromatography on a HiTrap chelating HP column (GE Healthcare), which was previously charged with 50 mM $NiSO_4$ and equilibrated with buffer A. The protein was eluted with buffer A containing 1 M imidazole. Figure 13 shows the elution profile from the HiTrap chelating HP column and SDS-PAGE of column fractions is shown in Figure 14. Secondly, gel filtration was performed on a HiLoad 16/600 Superdex 200 prep-grade column (GE Healthcare) with an elution buffer of 20 mM Tris-HCl at pH 8.5 and 100 mM NaCl. Figure 15 shows the elution profile of Superdex 200 column and SDS-PAGE of column fractions is displayed in Figure 16. Anion exchange chromatographic step was performed on HiTrap Q HP column, which was previously equilibrated with buffer (20 mM Tris-HCl at pH 8.5, 100 mM NaCl). VLR protein was eluted during sample loading (Figure 17). The purified proteins were homogeneous as judged by SDS-PAGE analysis (Figure 18).

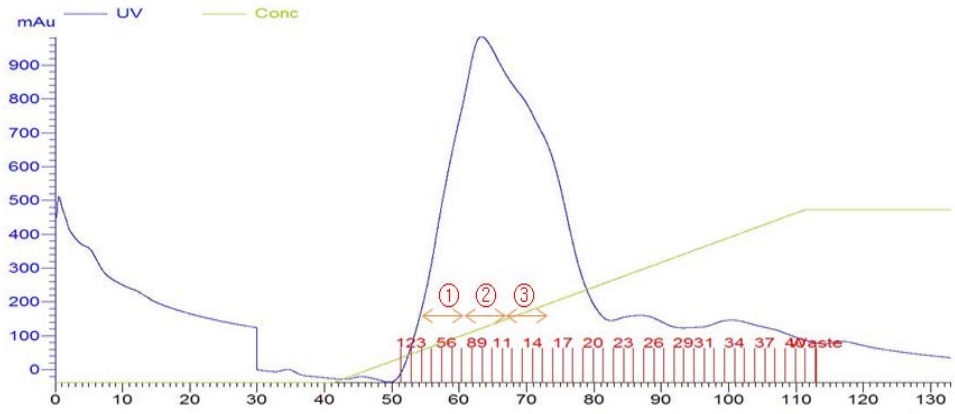

Figure 13. Elution profile from the HiTrap chelating HP column chromatography

Elution was performed with a linear gradient of 35 mM to 500 mM imidazole in 20 mM Tris-HCl at pH 7.5, and 500 mM NaCl

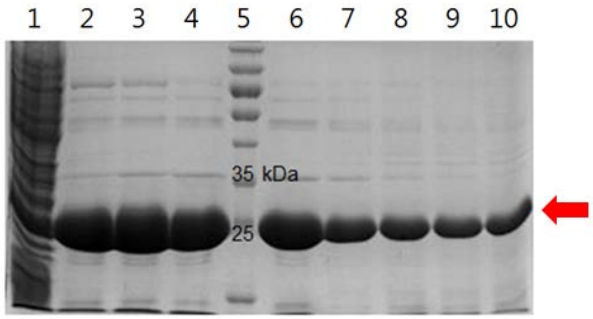

Figure 14. SDS-PAGE analysis of HiTrap chelating HP column fractions

Lane 1: Loading-thru
Lane 2: fraction #7
Lane 3: fraction #9
Lane 4: fraction #12
Lane 5: Protein marker (Fermentas)
Lane 6: fraction #14
Lane 7: fraction #19
Lane 8: fraction #24
Lane 9: fraction #29
Lane 10: fraction #31

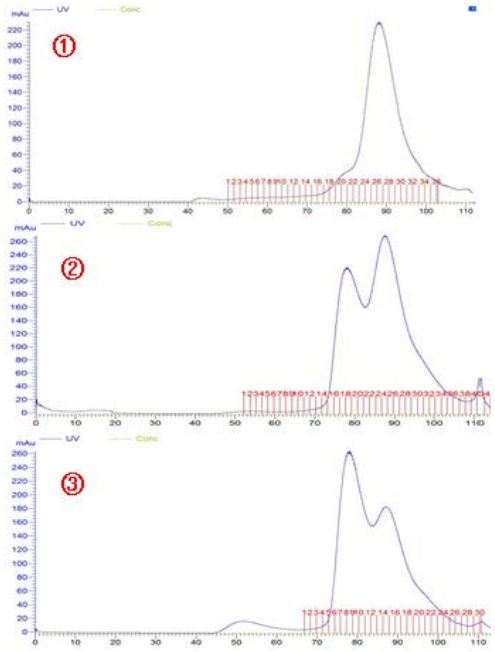

Figure 15. Elution profile from the Superdex-200 column chromatography

Elution was performed with 20 mM Tris-HCl at pH 8.5 and 100 mM NaCl

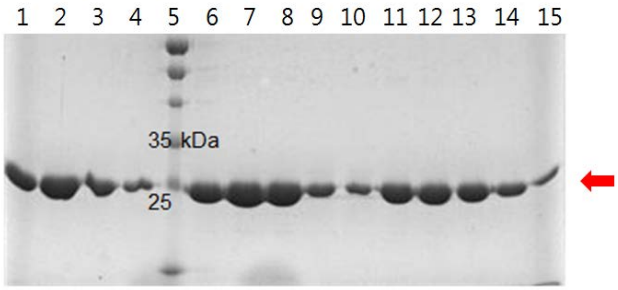

Figure 16. SDS-PAGE analysis of Superdex-200 column fractions

Lane 1: Elution profile① fraction #24
Lane 2: Elution profile① fraction #26
Lane 3: Elution profile① fraction #30
Lane 4: Elution profile① fraction #32
Lane 5: Protein marker (Fermentas)
Lane 6: Elution profile② fraction #22
Lane 7: Elution profile② fraction #24
Lane 8: Elution profile② fraction #26
Lane 9: Elution profile② fraction #30
Lane 10: Elution profile② fraction #32
Lane 11: Elution profile③ fraction #12
Lane 12: Elution profile③ fraction #13
Lane 13: Elution profile③ fraction #16
Lane 14: Elution profile③ fraction #19
Lane 15: Elution profile③ fraction #21

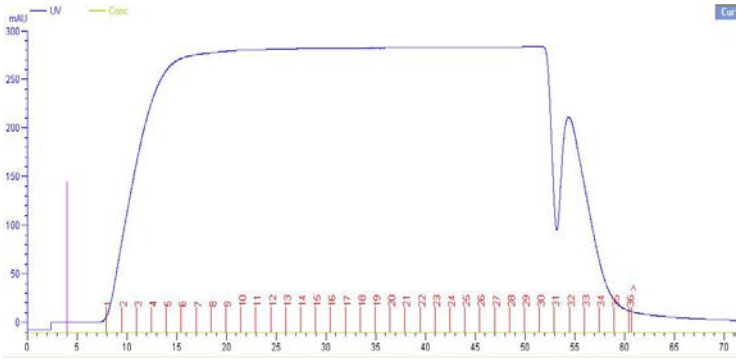

Figure 17. Elution profile from the HiTrap Q HP column chromatography

Elution was performed with a 100 mM NaCl in 20 mM Tris-HCl at pH 8.0

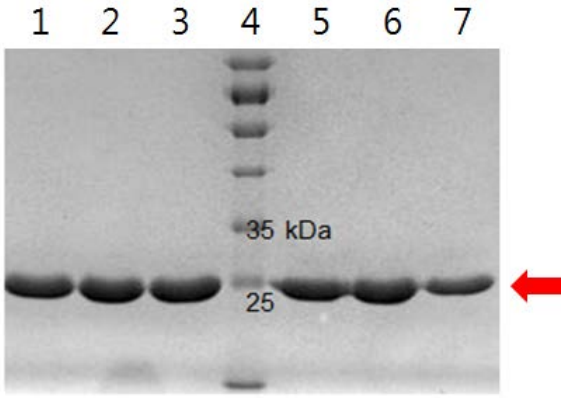

Figure 18. SDS-PAGE analysis of HiTrap Q HP column fractions

Lane 1: fraction #7
Lane 2: fraction #10
Lane 3: fraction #15
Lane 4: Protein marker (Fermentas)
Lane 5: fraction #18
Lane 6: fraction #22
Lane 7: fraction #27

4.1.3 InlB-VLR2913-ECD (A70D_N118D_D119Q_Y92F_N94C_D116A_ Y142F) Purification

The induced cells were harvested by centrifugation at 6,000 g for 10 min at 277 K. The wet cell weight was about 16.1 g for 4.5L culture. The cell pellets were lysed by sonication in buffer A (20 mM Tris-HCl at pH 7.5, 500 mM NaCl, 35 mM imidazole) containing 1 mM PMSF. The crude cell extract was centrifuged at 36,000 g for 1 hr at 277 K and the cell debris was discarded. The first step utilized the N-terminal hexa-histidine tag by affinity chromatography on a HiTrap chelating HP column (GE Healthcare), which was previously charged with 50 mM $NiSO_4$ and equilibrated with buffer A. The protein was eluted with buffer A containing 1 M imidazole. Figure 19 shows the elution profile from the HiTrap chelating HP column and SDS-PAGE of column fractions is shown in Figure 20. Secondly, gel filtration was performed on a HiLoad 16/600 Superdex 200 prep-grade column (GE Healthcare) with an elution buffer of 20 mM Tris-HCl at pH 8.5 and 100 mM NaCl. Figure 21 shows the elution profile of Superdex 200 column and SDS-PAGE of column fractions is displayed in Figure 22. Anion exchange chromatographic step was performed on HiTrap Q HP column, which was previously equilibrated with buffer (20 mM Tris-HCl at pH 8.5, 100 mM NaCl). VLR protein was eluted during sample loading (Figure 23). The purified proteins were homogeneous as judged by SDS-PAGE analysis (Figure 24).

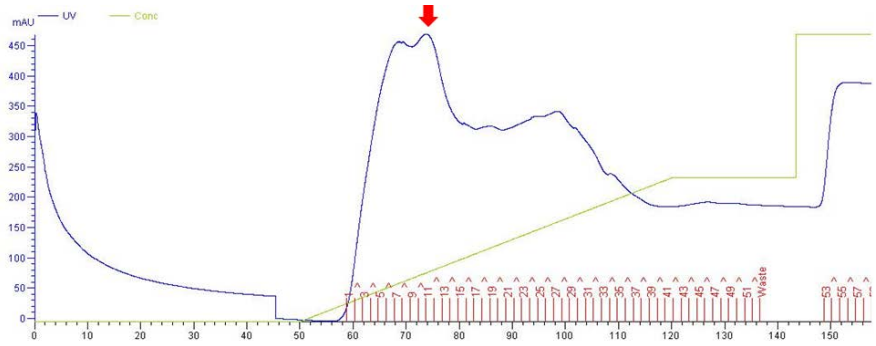

Figure 19. Elution profile from the HiTrap chelating HP column chromatography

Elution was performed with a linear gradient of 35 mM to 400 mM imidazole in 20 mM Tris-HCl at pH 7.5, and 500 mM NaCl

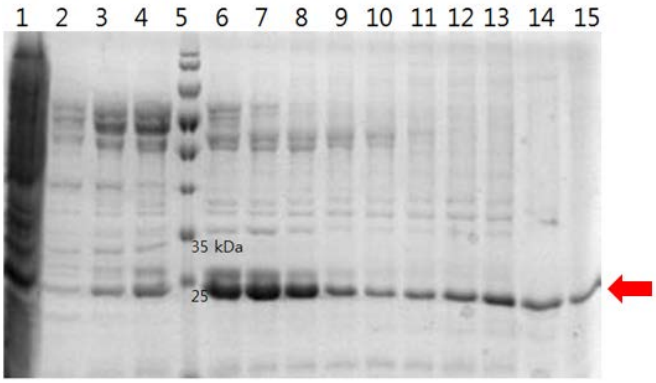

Figure 20. SDS-PAGE analysis of HiTrap chelating HP column fractions

Lane 1: Loading-thru
Lane 2: fraction #3
Lane 3: fraction #5
Lane 4: fraction #7
Lane 5: Protein marker (Fermentas)
Lane 6: fraction #11
Lane 7: fraction #13
Lane 8: fraction #15
Lane 9: fraction #17
Lane 10: fraction #19
Lane 11: fraction #23
Lane 12: fraction #27
Lane 13: fraction #31
Lane 14: fraction #35
Lane 15: fraction #47

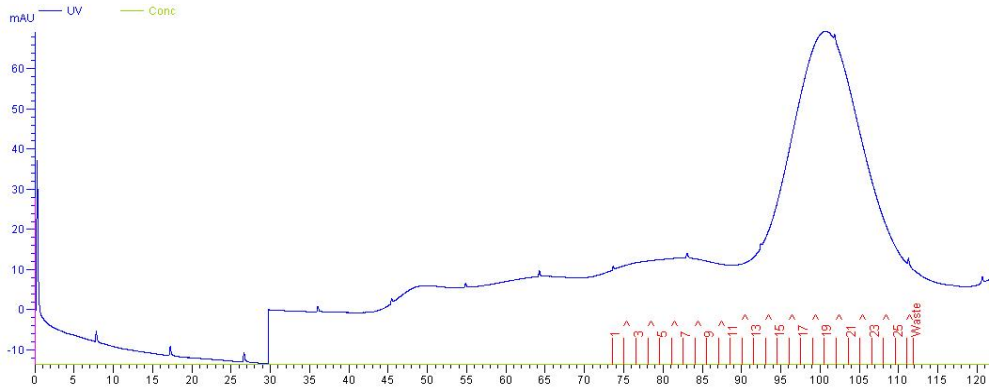

Figure 21. Elution profile from the Superdex-200 column chromatography

Elution was performed with 20 mM Tris-HCl at pH 8.5 and 100 mM NaCl

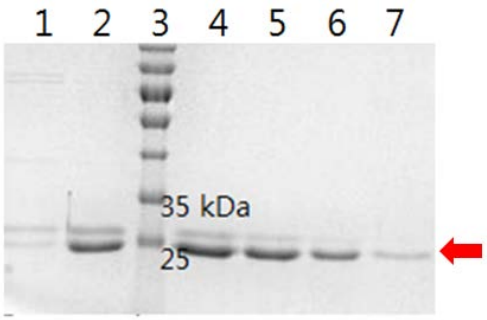

Figure 22. SDS-PAGE analysis of Superdex-200 column fractions

Lane 1: fraction #13
Lane 2: fraction #17
Lane 3: Protein marker (Fermentas)
Lane 4: fraction #19
Lane 5: fraction #21
Lane 6: fraction #23
Lane 7: fraction #25

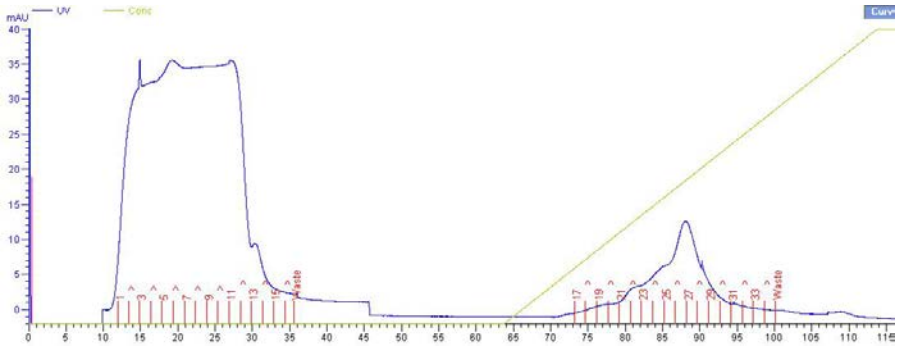

Figure 23. Elution profile from the HiTrap Q HP column chromatography

Elution was performed with a linear gradient of 100 mM to 700 mM NaCl in 20 mM Tris-HCl at pH 8.5

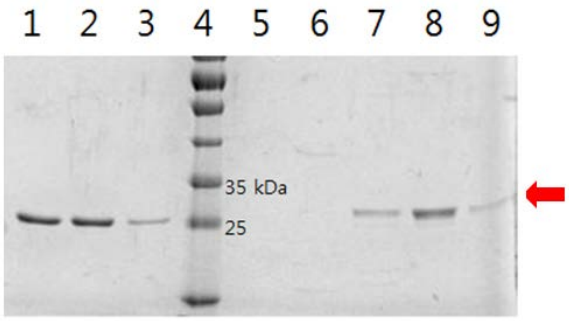

Figure 24. SDS-PAGE analysis of HiTrap Q HP column fractions

Lane 1: fraction #4
Lane 2: fraction #8
Lane 3: fraction #13
Lane 4: Protein marker (Fermentas)
Lane 5: fraction #19
Lane 6: fraction #22
Lane 7: fraction #25
Lane 8: fraction #27
Lane 9: fraction #29

4.2 InlB-VLR RBC36-ECD Purification

4.2.1 InlB-VLR RBC36-ECD (LRRV2-LRRCT) Purification

The induced cells were harvested by centrifugation at 6,000 g for 10 min at 277 K. The wet cell weight was about 15.5 g for 4.5L culture. The cell pellets were lysed by sonication in buffer A (20 mM Tris-HCl at pH 7.5, 500 mM NaCl, 35 mM imidazole) containing 1 mM PMSF and 5% glycerol. The crude cell extract was centrifuged at 36,000 g for 1 hr at 277 K and the cell debris was discarded. The first step utilized the N-terminal hexa-histidine tag by affinity chromatography on a HiTrap chelating HP column (GE Healthcare), which was previously charged with 50 mM $NiSO_4$ and equilibrated with buffer A. The protein was eluted with buffer A containing 1 M imidazole. Figure 25 shows the elution profile from the HiTrap chelating HP column and SDS-PAGE of column fractions is shown in Figure 26. Secondly, gel filtration was performed on a HiLoad 16/600 Superdex 200 prep-grade column (GE Healthcare) with an elution buffer of 20 mM Tris-HCl at pH 8.5 and 100 mM NaCl. Figure 27 shows the elution profile of Superdex 200 column and SDS-PAGE of column fractions is displayed in Figure 28. Anion exchange chromatographic step was performed on HiTrap Q HP column, which was previously equilibrated with buffer (20 mM Tris-HCl at pH 8.5, 100 mM NaCl). VLR protein was eluted during sample loading (Figure 29). The purified proteins were homogeneous as judged by SDS-PAGE analysis (Figure 30).

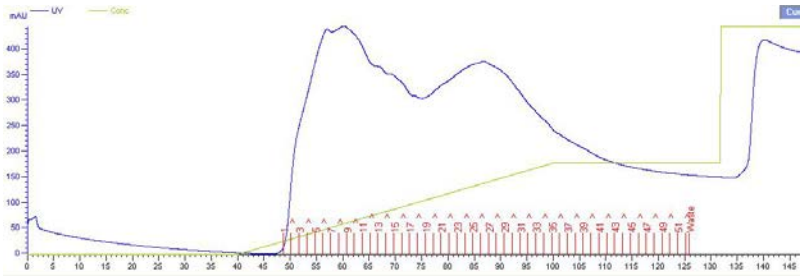

Figure 25. Elution profile from the HiTrap chelating HP column chromatography

Elution was performed with a linear gradient of 35 mM to 400 mM imidazole in 20 mM Tris-HCl at pH 7.5, and 500 mM NaCl

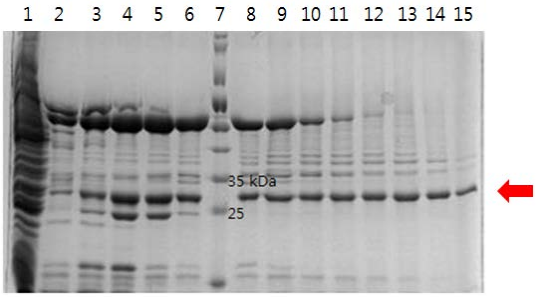

Figure 26. SDS-PAGE analysis of HiTrap chelating HP column fractions

Lane 1: Loading-thru
Lane 2: fraction #5
Lane 3: fraction #7
Lane 4: fraction #9
Lane 5: fraction #11
Lane 6: fraction #13
Lane 7: Protein marker (Fermentas)
Lane 8: fraction #15
Lane 9: fraction #17
Lane 10: fraction #19
Lane 11: fraction #21
Lane 12: fraction #27
Lane 13: fraction #31
Lane 14: fraction #35

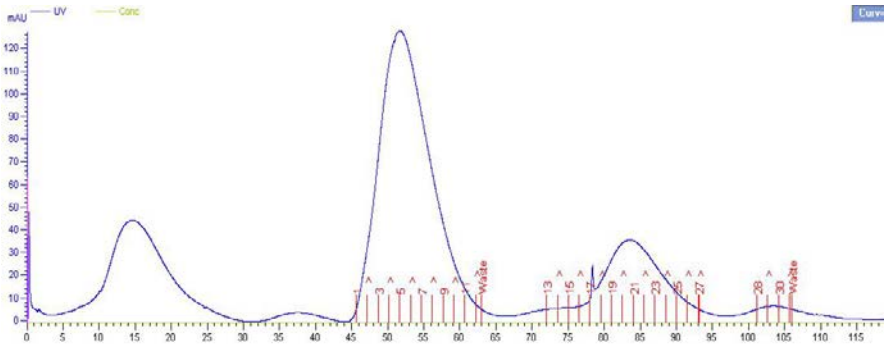

Figure 27. Elution profile from the Superdex-200 column chromatography

Elution was performed with 20 mM Tris-HCl at pH 8.5 and 100 mM NaCl

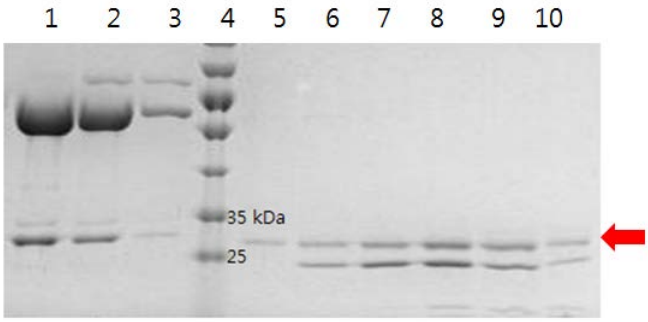

Figure 28. SDS-PAGE analysis of Superdex-200 column fractions

Lane 1: fraction #5
Lane 2: fraction #7
Lane 3: fraction #10
Lane 4: Protein marker (Fermentas)
Lane 5: fraction #15
Lane 6: fraction #17
Lane 7: fraction #18
Lane 7: fraction #21
Lane 7: fraction #23
Lane 7: fraction #25

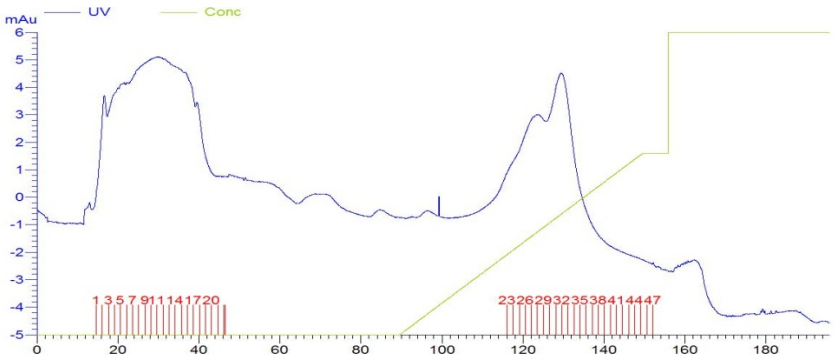

Figure 29. Elution profile from the HiTrap Q HP column chromatography

Elution was performed with a linear gradient of 100 mM to 600 mM NaCl in 20 mM Tris-HCl at pH 8.5

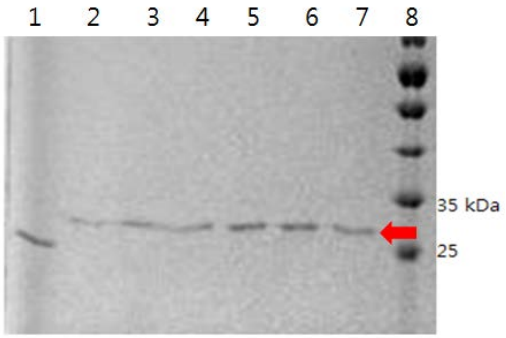

Figure 30. SDS-PAGE analysis of HiTrap Q HP column fractions

Lane 1: fraction #9
Lane 2: fraction #26
Lane 3: fraction #27
Lane 4: fraction #28
Lane 5: fraction #31
Lane 6: fraction #32
Lane 7: fraction #35
Lane 8: Protein marker (Fermentas)

5. Crystallization

InlB-VLR2913-ECD (A70D_N118D_D119Q) crystals were obtained by the sitting-drop vapour-diffusion method at 295K with reservoir solution consisting of 0.17 *M* ammonium sulfate, 25.5% (w/v) PEG4000, and 15% (v/v) glycerol (Figure 31).

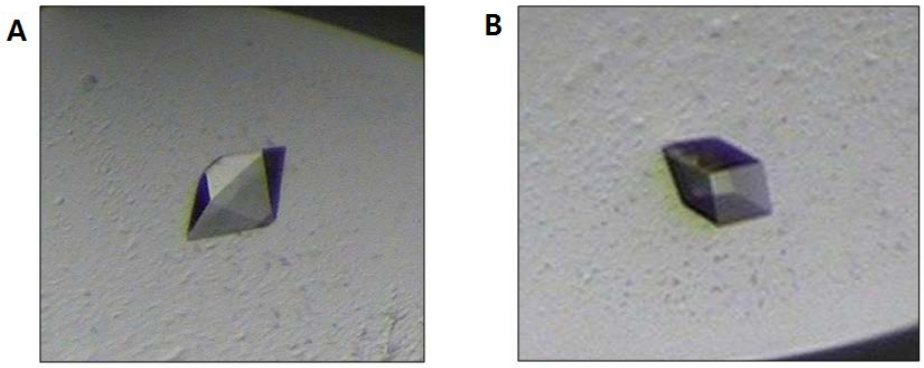

Figure 31. Initial hit (A) and optimized crystal (B) of the InlB-VLR2913-ECD (A70D_N118D_D119Q)

6. X-ray data collection

X-ray diffraction data were collected to 2.04 Å resolution (Figure 32) and indexed in a tetragonal space group. A total of 132,286 measured reflections were merged into 17,451 unique reflections, giving an R_{merge} of 5.2% and a completeness of 99.9%. The space group was determined to be $P4_12_12$ (or $P4_32_12$) on the basis of systematic absences and symmetry. The unit cell parameters were a = 91.12 Å, b = 91.12 Å, c = 62.87 Å (Table 2). If it is assumed that one monomer molecule is present in the crystallographic asymmetric unit, the calculated Matthews' coefficient (V_M) is 2.75 $Å^3$ Da^{-1} and the solvent content is 55.2%.

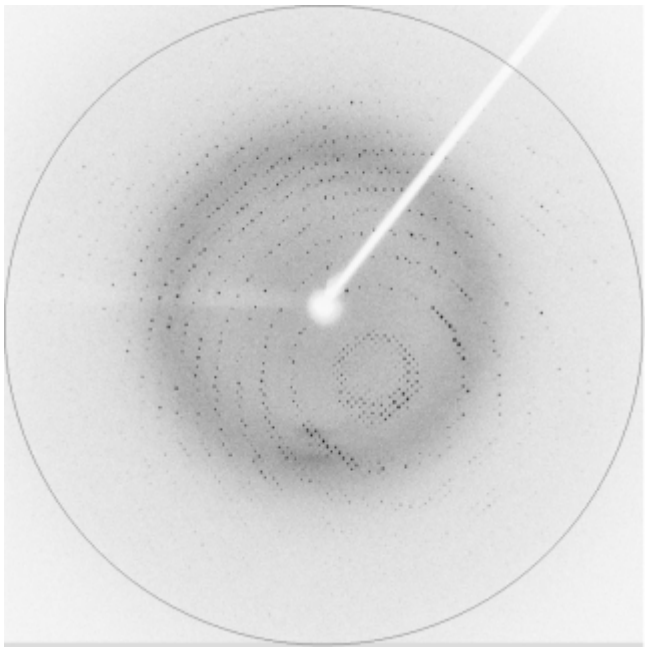

Figure 32. X-ray diffraction image from an InlB-VLR2913-ECD (A70D_N118D_D119Q) crystal.

The edge of the detector corresponds to a resolution of 2.04 Å and is represented as a circle. The detector distance was 150 mm and the exposure time for data collection was 3 minutes per image

InlB-VLR2913-ECD A70D_N118D_D119Q	
X-ray wavelength (Å)	1.54178
Temperature (K)	100
Space group	$P4_12_12$ ($P4_32_12$)
Unit cell parameters (Å)	$a = 91.12$, $b = 91.12$, $c = 62.87$
Resolution range (Å)	50-2.04 (2.08-2.04)
Total/unique reflections	132,286/17,451
R_{merge}† (%)	5.2 (32.1)
Data completeness (%)	99.9 (100)
Redundancy	7.6 (7.3)
Average $I/\sigma(I)$	44.6 (8.2)

Table 2. Data-collection statistics for InlB-VLR2913-ECD (A70D_N118D_D119Q)

†$R_{merge} = \Sigma_{hkl}\Sigma_i \mid I_i(hkl) - \langle I(hkl)\rangle \mid / \Sigma_{hkl}\Sigma_i I_i(hkl)$, where $I_i(hkl)$ is the intensity of the *i*th measurement of reflection *hkl* and $\langle I(hkl)\rangle$ is the average intensity of reflection *hkl*.

Values in parentheses are for the highest resolution shell.

7. Structure determination

The crystal structure of InlB-VLR2913-ECD (A70D_N118D_D119Q) was solved using molecular replacement (MR) program Molrep-autoMR with two search model (Protein Data Bank, PDB ID: 3RFJ and 2R9U) as search model (Figure 33, 34).

Figure 33. Overall structure of InlB-VLR2913-ECD (A70D_N118D_D119Q)

Red is N-terminus of Internalin B and yellow is VLR2913 ectodomain.

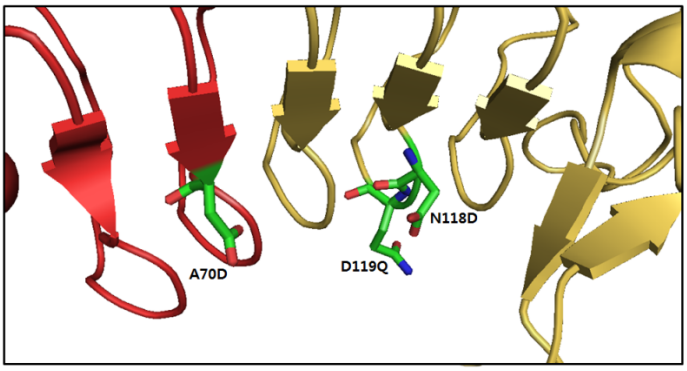

Figure 34. View concave surface of InlB-VLR2913-ECD (A70D_N118D_D119Q)

Green sticks in concave surface show three mutated residues.

8. Isothermal Titration Calorimetry 200

In binding affinity experiment by ITC200, the wild type and 3 residues mutant form (A70D_N118D_D119Q involved in hydrogen bonds) of InlB-VLR2913-ECD were not interacted with H-trisaccharide (Figure 35). It means that InlB-VLR2913-ECD requires additional factor for H-trisaccharide recognition. I confirmed an interaction between InlB-VLR2913-ECD with 7 residues mutation (A70D_N118D_D119Q_Y92F_N94C_D116A _Y142F involved in hydrogen bonds and van der Waals interaction) and H-trisaccharide (Figure 36).

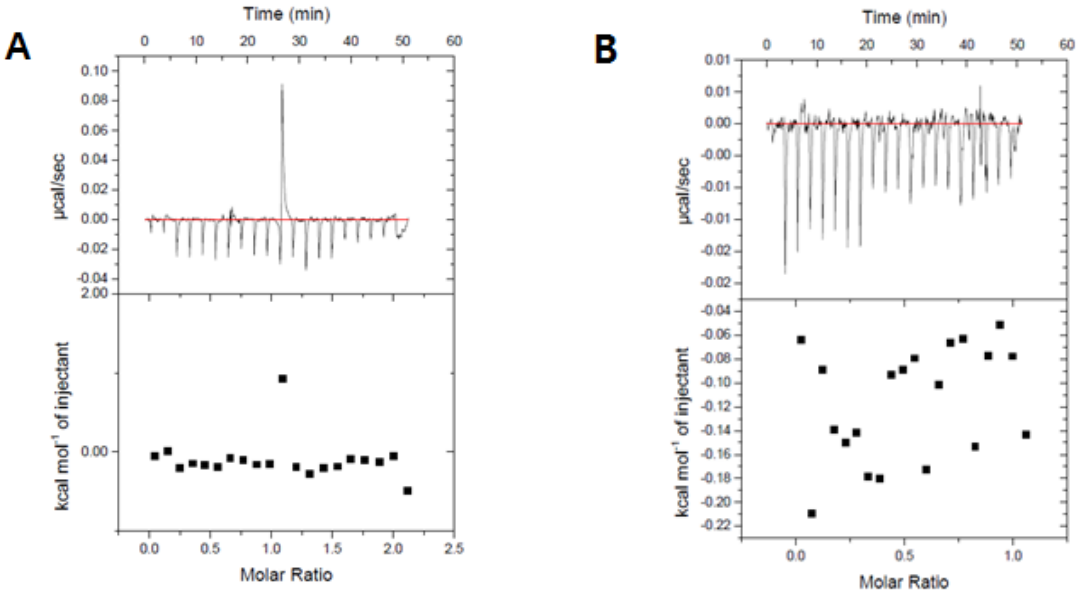

Figure 35. ITC data of InlB-VLR2913-ECD and H-trisaccharide

A) InlB-VLR2913-ECD (Wild type)
B) InlB-VLR2913-ECD (A70D_N118D_D119Q)

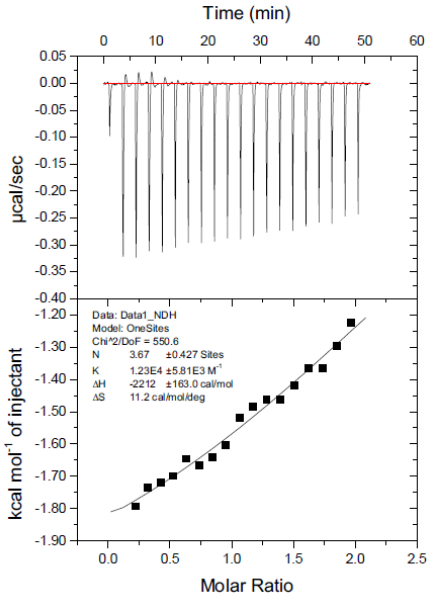

Figure 36. ITC data of InlB-VLR2913-ECD (A70D_N118D_D119Q_Y92F_N94C _D116A_Y142F) and H-trisaccharide

IV. References

1. Pancer Z, Amemiya CT, Ehrhardt GR, Ceitlin J, Gartland GL, Cooper MD. Somatic diversification of variable lymphocyte receptors in the agnathan sea lamprey. Nature 2004;430(6996):174-180.
2. Alder MN, Rogozin IB, Iyer LM, Glazko GV, Cooper MD, Pancer Z. Diversity and function of adaptive immune receptors in a jawless vertebrate. Science 2005;310(5756):1970-1973.
3. Pancer Z, Saha NR, Kasamatsu J, Suzuki T, Amemiya CT, Kasahara M, Cooper MD. Variable lymphocyte receptors in hagfish. Proceedings of the National Academy of Sciences of the United States of America 2005;102(26):9224-9229.
4. Han BW, Herrin BR, Cooper MD, Wilson IA. Antigen recognition by variable lymphocyte receptors. Science 2008;321(5897):1834-1837.
5. Velikovsky CA, Deng L, Tasumi S, Iyer LM, Kerzic MC, Aravind L, Pancer Z, Mariuzza RA. Structure of a lamprey variable lymphocyte receptor in complex with a protein antigen. Nature structural & molecular biology 2009;16(7):725-730.
6. Kim HM, Oh SC, Lim KJ, Kasamatsu J, Heo JY, Park BS, Lee H, Yoo OJ, Kasahara M, Lee JO. Structural diversity of the hagfish variable lymphocyte receptors. The Journal of biological chemistry 2007;282(9):6726-6732.
7. Tasumi S, Velikovsky CA, Xu G, Gai SA, Wittrup KD, Flajnik MF, Mariuzza RA, Pancer Z. High-affinity lamprey VLRA and VLRB monoclonal antibodies. Proceedings of the National Academy of Sciences of the United States of America 2009;106(31):12891-12896.
8. Herrin BR, Alder MN, Roux KH, Sina C, Ehrhardt GR, Boydston JA, Turnbough CL,

Jr., Cooper MD. Structure and specificity of lamprey monoclonal antibodies. Proc Natl Acad Sci U S A 2008;105(6):2040-2045.

9. Alder MN, Herrin BR, Sadlonova A, Stockard CR, Grizzle WE, Gartland LA, Gartland GL, Boydston JA, Turnbough CL, Jr., Cooper MD. Antibody responses of variable lymphocyte receptors in the lamprey. Nat Immunol 2008;9(3):319-327.

10. Pancer Z, Mariuzza RA. The oldest antibodies newly discovered. Nat Biotechnol 2008;26(4):402-403.

11. Deng L, Velikovsky CA, Xu G, Iyer LM, Tasumi S, Kerzic MC, Flajnik MF, Aravind L, Pancer Z, Mariuzza RA. A structural basis for antigen recognition by the T cell-like lymphocytes of sea lamprey. Proceedings of the National Academy of Sciences of the United States of America 2010;107(30):13408-13413.

12. Lee SC, Park K, Han J, Lee JJ, Kim HJ, Hong S, Heu W, Kim YJ, Ha JS, Lee SG, Cheong HK, Jeon YH, Kim D, Kim HS. Design of a binding scaffold based on variable lymphocyte receptors of jawless vertebrates by module engineering. Proceedings of the National Academy of Sciences of the United States of America 2012;109(9):3299-3304.

13. Otwinowski Z, Minor W. Processing of X-ray diffraction data collected in oscillation mode. Method Enzymol 1997;276:307-326.

V. Acknowledgments

I would like to express my gratitude to my research supervisor, Professor Byung Woo Han, for his kind advice during the course of this work. I am deeply grateful to my colleagues for their kind assistance and invaluable advice on this experiment.

국 문 초 록

VLR은 Variable Lymphocyte Receptor로서 척추동물 중에서 가장 하등하고 턱이 없는 무악류 척추동물의 적응면역체계이다. VLR의 Leucine-rich repeat (LRR) module의 concave surface와 LRRCT내에 있는 Highly Variable Insert (HVI)는 항원 인식에 다양성과 특이성을 제공한다. 특히 VLR들 간에 HVI의 서열 다양성은 매우 높다. 흔치 않게도, 혈액형 O형 사람이 가진 적혈구 표면에 존재하는 H항원의 H-trisaccharide를 인식하는 VLR RBC36와 아직 항원이 밝혀지지 않은 VLR2913의 HVI의 서열이 완전히 일치한다. 알려진 VLR들 사이에 HVI의 서열이 같은 경우는 매우 드물기 때문에 VLR2913 역시 H-trisaccharide를 인식할 것이라 예상하였다. 우리는 VLR2913의 항원을 밝히고, 특정 잔기가 돌연변이 된 VLR2913과 H-trisaccharide 사이에 결합친화도 실험을 통해 각각의 상호작용요소들이 항원인식에 기여하는 정도를 알아보고자 한다.

본 연구에서는 VLR2913의 박테리아 시스템을 이용한 단백질 발현을 위해 Internalin B가 N말단에 fusion된 재조합 VLR2913 ectodomain (InlB-VLR2913-ECD)을 제작하였고, VLR RBC36가 H-trisaccharide를 인식할 때 관여하는 수소결합과 반데르발스 상호작용에 기여하는 잔기들을 기반으로 VLR2913을 돌연변이 시켰다. 또한 박테리아 시스템을 이용해 대량 발현된 InlB-VLR2913-ECD를 affinity chromatography, size-exclusion chromatography와 ion exchange chromatography를 거쳐 순도 높은 InlB-VLR2913-ECD 단백질로 수백 조건의 결정화 스크리닝을 진행해 단백질 결정을 얻었고, X선을 이용해 2.04 Å resolution까지 diffraction data를 모아 구조를 규명했다. 또한 InlB-VLR2913-ECD와 H-trisaccharide의 상호작용 실험을 통해 VLR의 항원인식 관여요소들의 기여도를 보았다.

2011-21761